Numerical Simulation of Near-Critical and Unsteady, Subcritical Inlet Flow

R. W. Newsome*
Air Force Wright Aeronautical Laboratories, Wright-Patterson Air Force Base, Ohio

The unsteady, Reynolds-averaged Navier-Stokes equations were solved for the flow about an experimentally tested external compression axisymmetric inlet operating in the near-critical and unsteady subcritical flow regimes. The near-critical solution reached a stable steady state, while the subcritical solution attained an unstable, bounded oscillatory state characterized by large-amplitude pressure oscillations and traveling shock waves. The self-sustained oscillations, known as inlet buzz, result from a shear layer instability combined with a closed-loop feedback of reflected disturbances. Solutions are compared with experimental results.

Introduction

THE self-sustained oscillations encountered by supersonic inlets operating in the subcritical flow regime have been recognized as undesirable and potentially catastrophic since they were first observed by Oswatitsch.[1] The phenomenon is commonly known as inlet buzz and the characteristic large-amplitude pressure oscillations and traveling shock waves can result in structural damage, engine surge, combustion flameout, or nonrecoverable thrust loss. Inlet buzz has since been studied both experimentally and analytically.[2-6] Although these efforts have identified many salient features, the underlying physical mechanisms are still not well understood. At present there is no satisfactory method for predicting buzz onset or the amplitude and frequency of the resulting oscillations.

Recent advances in computers and computational methods have enabled the direct numerical simulation of unsteady flows exhibiting self-sustained oscillations. To date, results have been reported for transonic airfoil,[7] aileron,[8] cavity,[9] spike-tipped body,[10] cylinder,[11] and supercritical diffuser[12] flows. The objective of this effort was to similarly investigate the utility of computational methods as a tool for the prediction and understanding of subcritical inlet buzz.

Theoretical Considerations

A better understanding of inlet buzz is afforded by a brief review of related theoretical work. Rockwell and Naudasher[13] and Hankey and Shang[14] have outlined necessary conditions for a self-sustained oscillation to occur:

1) Selective amplification of disturbances in an unstable shear layer over a limited frequency range.

2) Upstream feedback of reflected disturbances from a downstream impingement surface to the unstable shear layer in proper phase and at a frequency where amplification is possible.

These mechanisms are present in inlet buzz as well.

Shear-Layer Instability

A separated boundary layer provides the necessary fluid dynamic amplifier for inlet buzz. The separated flow contains a point of inflection in the velocity profile. Such profiles are known to be unstable (Rayleigh's first theorem) and spatial stability theory has been used to show that the separated region will amplify disturbances over a narrow frequency range. Early studies[2,4] suggested the separation may be shock induced or may result from shock-generated vortex sheet impingement on the cowl wall.

Feedback Mechanism

The dominant feedback mechanism for the inlet considered is the reflection of compression and expansion waves in like sense from the choked exit throat. The buzz cycle begins with the forward expulsion of the bow shock on the centerbody and a consequent expansion wave that propagates downstream. The reflected expansion wave interacts with the bow shock and the shock retreats inward. This generates a compression wave that similarly travels downstream and is reflected to expel the bow shock and begin the cycle gain.

For flow along an inlet of length L, at an average Mach number M, the fundamental period of the oscillation is given as

$$P=4L/(1-M^2)c \tag{1}$$

where c is the speed of sound. The fundamental frequency and higher frequency modes f_N as predicted for a duct with an open and a closed end are

$$f_N=\frac{1}{P}(2N-1)=\frac{c}{4L}(1-M^2)(2N-1) \quad N=1,2,3\ldots \tag{2}$$

Method of Solution

Since the problem is characterized by large separated regions in an unsteady, turbulent flow with strong viscous-inviscid interaction, the relevant equations are the axisymmetric Reynolds-averaged Navier-Stokes equations as given in Ref. 15. The equations were closed by the perfect gas equation of state, Sutherland's law, Stokes's hypothesis, and a Cebeci-Smith[16] algebraic model for the turbulent eddy viscosity. Although this particular model has known deficiencies for separated flows with large adverse pressure gradients, the superiority of more complex models has not been conclusively demonstrated. The algebraic model was adopted to provide an approximate representation of the turbulence at a reasonable computational cost.

A simple algebraic scheme was used to generate a grid to solve for both internal and external flows about the inlet. A typical grid for the upstream region is shown in Fig. 1. Minimum spacing in the radial direction was set by a uniform step size at the cowl lip and maintained along the length of the

Presented as Paper 83-0175 at the AIAA 21st Aerospace Sciences Meeting, Reno, Nev., Jan. 10-13, 1983; submitted April 7, 1983; revision received Dec. 20, 1983. This paper is declared a work of the U.S. Government and therefore is in the public domain.

*Captain, USAF; Aerospace Engineer. Member AIAA.

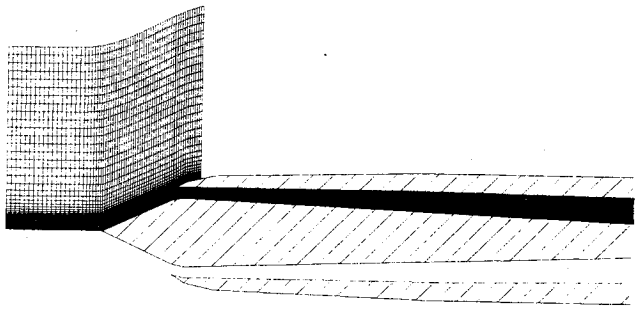

Fig. 1 Forebody grid used in buzz calculations.

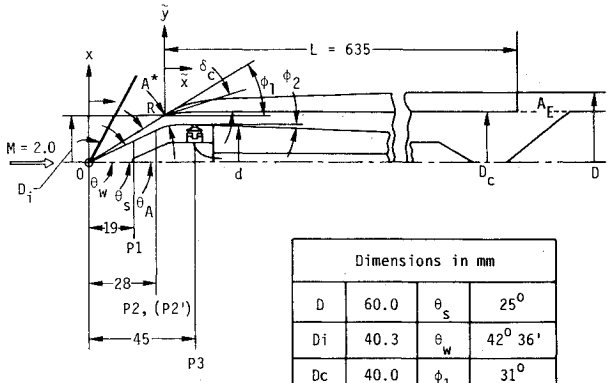

Dimensions in mm			
D	60.0	θ_s	25°
Di	40.3	θ_w	42° 36'
Dc	40.0	ϕ_1	31°
d	32.4	δ_c	19° 24'
R	0.05	ϕ_2	2° 18'
		θ_A	31° 35'

Fig. 2 Inlet model characteristics (Ref. 5).

inlet. This produced an exponentially stretched grid near the walls, blended to a constant step size in the interior of the duct.

MacCormack's[17] explicit finite difference algorithm was chosen for numerical integration of the governing equations based on its robustness, its time-accurate resolution, and its efficient implementation on a vector processor computer.

Freestream boundary conditions were applied for the supersonic inflow boundary, which was placed far enough upstream to contain the forward travel of the shock. A symmetry condition was specified on the centerline in front of the centerbody. On the solid walls, temperature was specified together with the no-slip velocity condition. A simplified compatibility condition for pressure completed the surface boundary condition definition. The outer exterior boundary was updated using a characteristic extrapolation along the outward running characteristic. Properties at the downstream boundary for both internal and external flows were extrapolated. As a consequence of the domain of dependence, this boundary condition had no influence on the upstream solution for supersonic flow. For the cases considered, the exit throat remained choked. The choked throat was a sufficient downstream constraint, both physically and numerically. It sufficed to position the shock within the duct and also correctly reflected the rearward traveling expansion and compression waves. A divergent section was appended to the throat in order to accelerate the flow to a supersonic exit state where the boundary condition was applied. This artifice insured that the solution was free from numerical boundary condition influence.

Initial conditions were prescribed as various combinations of one-dimensional inviscid solutions, previously computed solutions, and stagnation conditions for cases where the exit throat was closed.

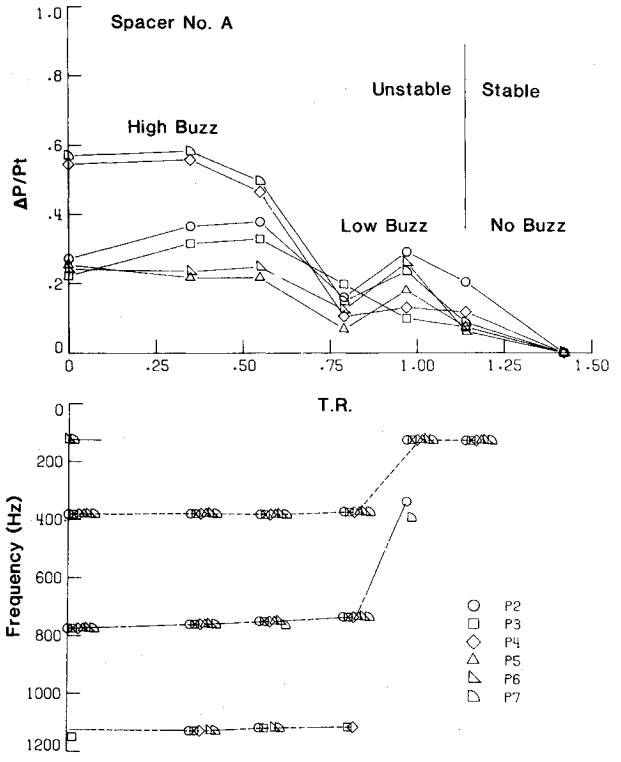

Fig. 3 Amplitude and frequency characteristics of experimental pressure oscillations (Ref. 5).

All calculations were performed on the CRAY 1-S computer with the vectorized algorithm. The resulting rate of data processing (RDP) was

$$\text{RDP} = \frac{\text{CPU time, s}}{\text{(No. grid points)(No. iterations)}} = 1.74 \times 10^{-5} \text{ s}$$

Results

Experimental Results

An external compression axisymmetric inlet with a length-to-diameter ratio, $L/D = 15.88$, tested experimentally by Nagashima et al.[5] was chosen for comparison. Inlet geometry is given in Fig. 2. Test conditions corresponded to a Mach 2 freestream with a Reynolds number based upon diameter, $Re_D = 2.36 \times 10^6$ ($D = 6$ cm), at 3 atm total pressure. Instrumentation consisted of high-speed schlieren photography of the exterior flow, seven high response static pressure probes (P1-P7, see Fig. 5), and a spectral analyzer for frequency analysis of the waveforms.

Results were obtained for throttle ratios, $TR = A_e/A_c$, corresponding to supercritical, critical, and subcritical conditions by changing the position of a throttle valve at the exit. A_c is the minimum cross-sectional area at the cowl lip. A_e is the flow exit area through the sides of the cowl walls and is not the minimum cross-sectional area at which the flow is choked. For throttle ratios above $TR = 1.14$ the flow was steady, while smaller values resulted in buzz. Amplitude and frequency characteristics at the seven probe locations are summarized in Fig. 3. At higher subcritical throttle ratios, a low-amplitude oscillation with a dominant fundamental frequency was observed. At much smaller values, a higher amplitude oscillation with a dominant frequency component three times the fundamental was found (see Table 1).

Typical waveforms are shown in Fig. 4.

Numerical Results

Numerical results are presented for one steady-state, near-critical solution and two solutions corresponding to high and

Table 1 Dominant frequency (from spectral analysis) and corresponding linear frequency mode

Experiment	Theory [Eq. (2)]
$TR=0.97$ $f=110$ Hz	$f_1=110$ Hz for $M=0.36$
$TR=0.0$ $f\simeq 391$ Hz	$f_3=381$ Hz for $M=0.0$

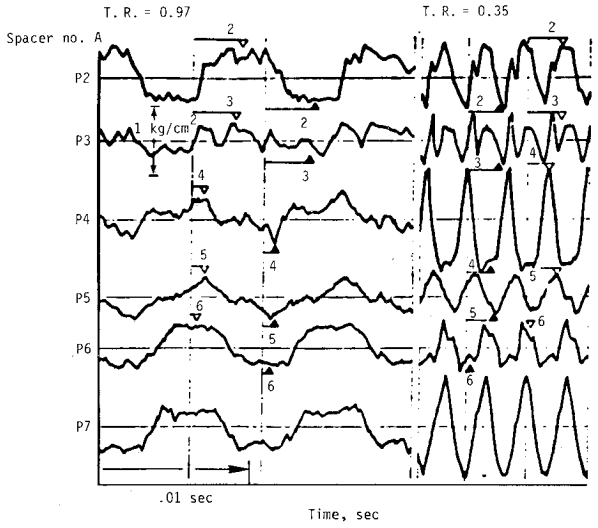

Fig. 4 Experimental pressure fluctuations (Ref. 5).

low subcritical throttle ratios. Minor changes in the exit throat geometry were made to correctly impose the choked exit flow condition. Results were correlated in terms of an area ratio $AR=A_*/A_c$, where A_* is the actual experimental choking area. The computed inlet geometry and experimental pressure probe locations are shown in Fig. 5. Grid dimensions were 190 axial points and 30 interior and 64 exterior radial points. The turbulent nondimensional step size adjacent to the wall was typically $y_+\approx 40$. This rather coarse viscous resolution was necessary in order to obtain reasonable run times for the very long oscillation time period with the present explicit method.

Near-Critical Steady State ($TR=1.42$, $AR=1.16$)

Turbulence was assumed to be abruptly triggered by the normal shock with fully turbulent flow shortly downstream of this point. The flow reached a steady state in which the normal shock position was determined as a consequence of shock and viscous total pressure losses, together with the required continuity of mass at the entrance and exit sections. Mach contours at the inlet region may be compared with experimental schlieren results in Fig. 6. A comparison of static pressure on the cowl and centerbody with experiment is given in Fig. 7. Consistent with the gradual pressure rise, a region of three lip duct heights was observed in which the Mach number oscillated from 1.1 to 0.9 immediately behind the initial terminal shock. The jump conditions for an ideal normal shock were not attained until some 7.6 cowl lip duct heights over 28 axial grid stations downstream. This deviation from ideal shock behavior is not numerically induced, but is a result of shock/boundary-layer interaction in which a single normal shock is replaced by a series of weak bifurcated normal shocks. Much finer grid resolution would be required to resolve the detailed structure of this region.

Subcritical Flow ($TR=0.97$, $AR=0.83$)

Although buzz was not found numerically at this condition, some insight was gained as to the nature of the instability. Turbulent transition was again set immediately aft of the

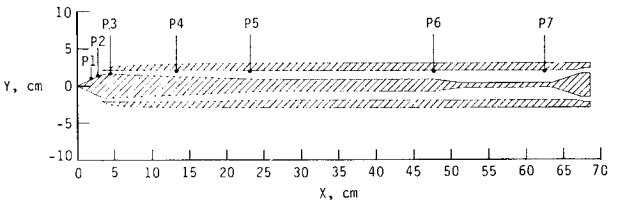

Fig. 5 Computed inlet geometry with experimental static pressure probe locations ($TR=1.42$, $AR=1.16$, $L/D=15.88$).

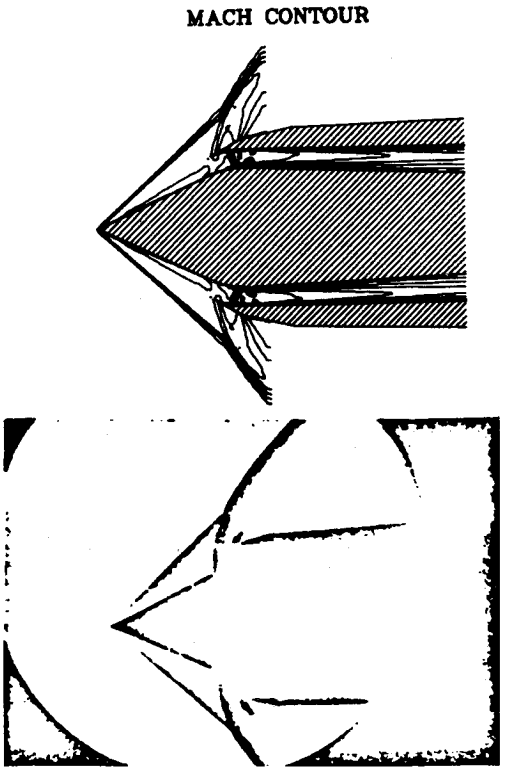

Fig. 6 Forebody flow: computation vs schlieren photograph, steady flow ($TR=1.42$, $AR=1.16$).

normal shock and the solution started with an impulsive decrease in exit throat area. This generated a compression wave that traveled forward to expel the shock from the interior. The solution converged to a steady state corresponding to the experimentally observed maximum pressure level at buzz onset. Since the flow was separated in only a small region on the centerbody, the resulting steady-state solution is consistent with the hypothesis that a large separated region is a necessary condition for buzz. In order to produce a larger separated region more subject to disturbance amplification, the onset of transition from laminar to turbulent flow was specified at 6 cm ($Re_x=2.3\times 10^6$) and fully turbulent flow was set at 12 cm ($Re_x=4.7\times 10^6$). The laminar region was less able to withstand the adverse pressure gradient and separated on both the centerbody and cowl. As expected, the flow was no longer steady and the bow shock moved forward in response to flow blockage within the inlet produced by the unsteady separated boundary layers. This is in accord with earlier theories[2,4] where the instability was triggered by massive boundary-layer-induced flow blockage. However, unsteadiness remained localized in the laminar region near the lip and the globally organized buzz motion did not develop. Although the diffuser flow was almost certainly turbulent, the turbulence model appeared to artificially damp the instability. Experimentally, due to slight eccentricity in the centerbody position, the shock structure was asymmetric. Given the

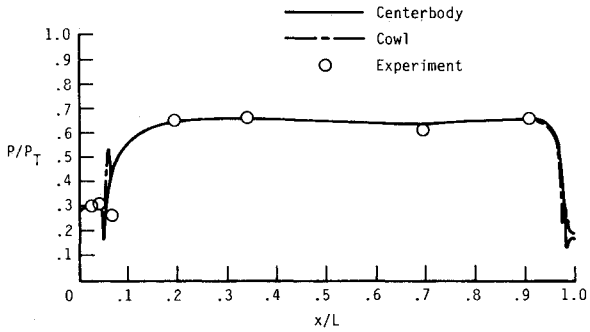

Fig. 7 State pressure distribution ($TR = 1.42$, $AR = 1.16$).

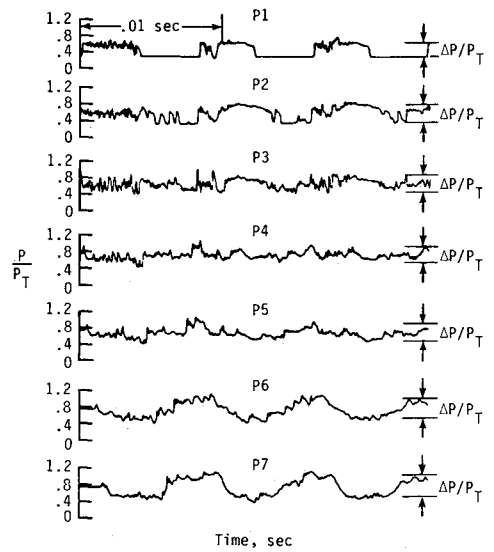

Fig. 8 Computed pressure fluctuations for experimental probe locations of Fig. 5 ($TR = 0.0$).

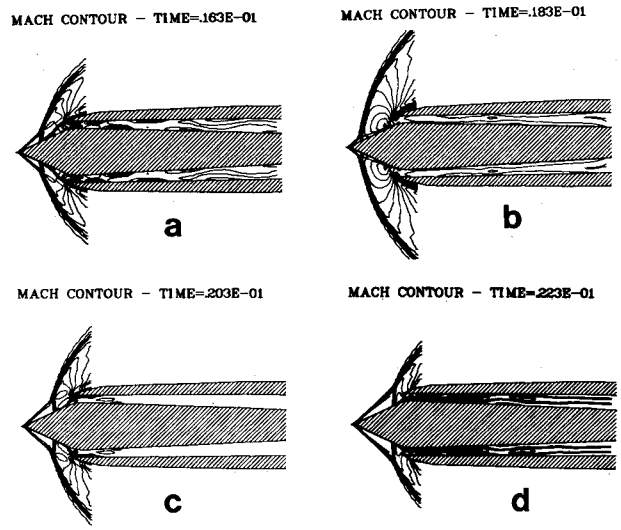

Fig. 9 Forebody flow: third buzz cycle at selected time intervals, in seconds ($TR = 0.0$).

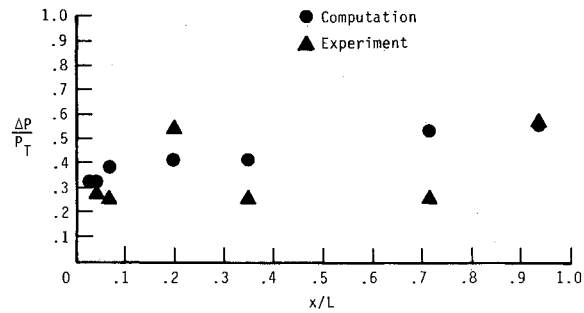

Fig. 10 Amplitude of experimental and computed pressure fluctuations at experimental probe locations ($TR = 0.0$).

sensitivity to turbulence modeling and the asymmetry, which could not be accounted for with axisymmetric equations, further calculations were not attempted for this throttle ratio.

Subcritical Flow ($TR = 0.0$)

A flow condition corresponding to a closed throat was chosen as representative of the low-mass flow regime. Initial conditions assumed a stagnation state within the inlet. Because the turbulence model had previously been found to damp the occurrence of the instability, it was not applied in the present case. A plausible justification for this omission depends upon several assumptions. Spectral analysis of the experimental waveforms revealed a large-scale organized motion with discrete low-frequency peaks and a broader band of higher turbulent frequencies. When applied to unsteady, oscillatory flows, the turbulence model should properly account only for the higher frequencies that cannot be resolved on the grid. Existing turbulence models, derived from stationary data bases, may overpredict the appropriate eddy viscosity. If the turbulence model is omitted, the turbulence transport processes are to a limited extent resolvable, but the dissipative processes are not. Shang[11] has recently shown that solutions to the laminar Navier-Stokes equations can reproduce some "large-scale" turbulent statistical properties for an unsteady oscillatory flow in the transitional Reynolds number range.

Under these assumptions, a numerical solution was computed for three complete buzz cycles. The calculation required 3.75 h of CPU time on the CRAY 1-S. The instability developed immediately as a consequence of the non-equilibrium state of the initial conditions. Pressure-time traces at the seven experimental probe locations are shown in Fig. 8. It should be noted that the amplitude exhibits no significant growth or decay over the three computed cycles. The step-like behavior of the dominant fundamental mode is obvious at all stations except near the cowl lip. The period associated with this motion ($P = 0.0078$ s) can be determined by evaluating the interval required for the shock to cross the probe P1 on successive cycles. The calculated frequency was 128 Hz, which is very close to the theoretical fundamental frequency, $f_1 = 127$ Hz, obtained from Eq. (2) with $M = 0.0$. Additional higher-frequency modes were introduced by the unstable separated shear layers and are most evident in probes P3 and P4, where the waveform was highly erratic.

Several Mach contour plots representative of the third computed buzz cycle are shown in Fig. 9. During the first half of the buzz cycle, the bow shock was forced to the tip of the centerbody as a result of interaction with a reflected compression wave. In the expulsion phase, a region of reverse flow extended between the base of the bow shock and the cowl lip. The shear layer dividing the two regions can be seen in Fig. 9a. As the shock reached the centerbody tip, the shear layer ruptured and the flow spilled radially outward. The bow shock remained in this position for a period of time corresponding to the propagation and reflection of an expansion wave. At this time (Fig. 9c), the inlet began to ingest mass and the shock retreated to a position just forward of the cowl lip. During the ingestion phase, several regions of separated flow (Fig. 9d) located on the centerbody and cowl in an alternating fashion are clearly visible immediately downstream from the cowl lip.

The only experimental information available for this case appears in Fig. 3. The experiment displayed a frequency shift equivalent to the third and higher modes, except at the two downstream probes where the fundamental mode was also observed. The computation, however, revealed a dominant fundamental mode similar to the experimental case, $TR = 0.97$ (Fig. 4), in both the waveform and phase relationships. Because the waveforms were different, the point-by-point correspondence between experimental and numerical amplitudes (Fig. 10) is not particularly good. Although several hypotheses[4] such as vortex shedding or an edge tone phenomenon have been suggested to explain the experimental frequency shift, this mechanism is not presently understood.

Conclusions and Recommendations

A numerical method has been used to solve for the flow about an external compression axisymmetric inlet. The steady-state solution agreed well with all available experimental data. Investigations at the high subcritical throttle ratio, $TR = 0.97$, demonstrated a large sensitivity to turbulence modeling. Evidence was also found to support the hypothesis that the separated boundary layer plays an essential role in the instability mechanism. At the low subcritical throttle ratio, $TR = 0.0$, buzz was numerically computed with a dominant frequency corresponding to the fundamental mode predicted by a simple wave propagation model. The computed solution displayed large-amplitude pressure oscillations and traveling shock waves characteristic of inlet buzz. In addition, regions of separated flow exhibiting a high-frequency instability and the feedback mechanism of reflected pressure waves were shown. This work represents the first time the fundamental governing equations have been used to predict subcritical inlet buzz.

Further progress in the numerical simulation of inlet buzz depends upon resolution of several problem areas. The computational effort involved in the present solutions is a significant deterrent to a thorough investigation of the possible operating conditions and model assumptions. Practical simulations require an order of magnitude reduction in computer time. A second need is for a clearer understanding of the role of turbulence and turbulence modeling in the solution process. In particular, better models for unsteady, oscillatory, separated flows appear to be needed. Finally, there is a need for more detailed experimental work. Flow visualization and detailed measurements are invaluable in guiding and validating numerical results. In fact, numerical and experimental studies are complimentary and their joint use is recommended in future efforts to better understand inlet buzz.

Acknowledgments

This material is based on the author's dissertation in partial fulfillment of the requirements for the Doctor of Philosophy degree at the Air Force Institute of Technology, Wright-Patterson Air Force Base, Ohio. The technical guidance and advice of Dr. W. Hankey and Dr. J. Shang of the Air Force Wright Aeronautical Laboratories are greatefully acknowledged.

References

[1] Oswatitsch, K., "Pressure Recovery in Missiles with Reaction Propulsion at High Supersonic Speeds (The Efficiency of Shock Diffusers)," NACA TM-1140 (translation), June 1947.

[2] Ferri, A. and Nucci, R. M., "The Origin of Aerodynamic Instability of Supersonic Inlets at Subcritical Conditions," NACA RM-L50K30, Jan. 1951.

[3] Trimpi, R. L., "A Theory for Stability and Buzz Pulsation Amplitude in Ram Jets and an Experimental Investigation Including Scale Effects," NACA Rept. 1265, 1956.

[4] Dailey, C.L., "Supersonic Diffuser Instability," *Journal of the Aeronautical Sciences*, Vol. 22, Nov. 1955, pp. 733-749.

[5] Nagashima, T., Obokato, T., and Asanuma, T., "Experiment of Supersonic Air Intake Buzz," Institute of Space and Aeronautical Science, University of Tokyo, Japan, Rept. 481, May 1972.

[6] Sajben, M., Bogar, T. J., and Kroutil, J. C., "Experimental Study of Flows in a Two-Dimensional Inlet Model," AIAA Paper 83-0176, Jan. 1983.

[7] Levy, L. L., "Experimental and Computational Steady and Unsteady Transonic Flows about a Thick Airfoil," *AIAA Journal*, Vol. 16, June 1978, pp. 564-572.

[8] Steger, J. L. and Bailey, A. E., "Calculation of Transonic Aileron Buzz," *AIAA Journal*, Vol. 18, March 1980, pp. 249-255.

[9] Hankey, W. L. and Shang, J. S., "Analysis of Pressure Oscillations in an Open Cavity," *AIAA Journal*, Vol. 18, Aug. 1980, pp. 892-898.

[10] Shang, J. S., Hankey, W. L., and Smith, R. E., "Flow Oscillations of Spike Tipped Bodies," AIAA Paper 80-0062, Jan. 1980.

[11] Shang, J. S., "Oscillatory Compressible Flow Around a Cylinder," AIAA Paper 82-0098, Jan. 1982.

[12] Liou, M. S. and Coakley, T. J., "Numerical Simulation of Unsteady Transonic Flow in Diffusers," AIAA Paper 82-1000, June 1982.

[13] Rockwell, D. and Naudasher, E., "Self-Excited Oscillations of Impinging Free Shear Layers," *Annual Review of Fluid Mechanics*, Vol. 11, 1979, pp. 67-94.

[14] Hankey, W. L. and Shang, J. S., "Analysis of Self-Excited Oscillations in Fluid Flows," AIAA Paper 80-1346, July 1980.

[15] Newsome, R. W., "Numerical Solutions for Critical and Unsteady Subcritical Flow about an External Compression Axi-Symmetric Inlet," Ph.D. Dissertation, Air Force Institute of Technology, Wright-Patterson AFB, Ohio, Nov. 1982.

[16] Cebeci, T. and Smith, A. M. O., *Analysis of Turbulent Boundary Layers*, Academic Press, New York, 1974.

[17] MacCormack, R. W. and Baldwin, B. S., "A Numerical Method for Solving the Navier-Stokes Equations with Application to Shock-Boundary Interactions," AIAA Paper 75-1, Jan. 1975.